phys. stat. sol. (c) **0**, No. 2, 652–656 (2003) / **DOI** 10.1002/pssc.200306176

Donor-related density of states and polarizability in a GaAs-(Ga, Al)As quantum-well under hydrostatic pressure and applied electric field

A. L. Morales, A. Montes, S. Y. López, N. Raigoza, and **C. A. Duque**[*]

Instituto de Física, Universidad de Antioquia, AA 1226, Medellín, Colombia

Received 24 July 2002, accepted 14 August 2002
Published online 30 January 2003

PACS 71.55.Eq, 73.21.Fg, 78.67.De

Theoretical calculations have been used to assess the influence of both an external electric field and hydrostatic stress on the binding energy, impurity polarizability, as a function of the impurity position and density of states for shallow-donor impurities in a GaAs–(Ga, Al)As quantum well. The binding energy maximum is shifted toward the wall at $z = -L/2$ of the quantum well for increasing values of electric field (keeping a constant pressure) and increasing values of pressure (keeping a constant electric field). The polarizability follows closely the behavior of the binding energy so for smaller binding energies the polarizability is large showing a more delocalized electron cloud. Also, it has been observed that the density of states depends strongly on the applied hydrostatic stress and electric field. In the absence of an electric field the energy level is degenerate for symmetrical positions of the impurities with respect to the center of the quantum well. However, this degeneracy is broken when an electric field is applied in the growth direction of the structure. Associated with this, the density of states becomes richer in structure.

1. Introduction Studies of the effect of hydrostatic stress have proven to be invaluable in the context of the optical properties of semiconductors and their heterostructures [1–9]. For a given structure, the difference in energy between the type–I and –II transitions can be tuned with external hydrostatic pressure in a continuous and reversible manner. This makes possible an elucidation of the properties of various interband transitions.

The application of an electric field in the growth direction of the heterostructure gives rise to a polarization of the carrier distribution and to an energy shift of the quantum states. Such effects may introduce considerable changes in the energy spectrum of the carriers, which could be used to control and modulate the output of optoelectronic devices [10, 11]. Through the wave function, the polarizability measurements shed light on the dynamics of the carriers and optical properties in low dimensional heterostructures [12–16].

In previous work [17] we have calculated the binding energy and impurity polarizability, as a function of both electric field and hydrostatic stress, for a shallow-donor impurity at the center of the single GaAs–(Ga, Al)As quantum well (QW). Here we extend the previous findings considering the binding energy, the polarizability, as a function of the impurity position and the density of impurity states (DOIS) for a uniform distribution of impurities. In this paper we use a variational scheme within the effective mass approximation.

[*] Corresponding author: e-mail: cduque@fisica.udea.edu.co, Phone: 57-4-210 56 30, Fax: 57-4-233 01 20

© 2003 WILEY-VCH Verlag GmbH & Co. KGaA, Weinheim 0370-1972/03/00002-0652 $ 17.50+.50/0

2. Theoretical framework In the effective-mass approximation, the Hamiltonian for a hydrogenic shallow-donor impurity in a GaAs–$Ga_{1-x}Al_xAs$ QW (with L_0 size at zero hydrostatic pressure), under the effect of a hydrostatic pressure (P) and electric field (F), in the z-direction, is given by [17]

$$H = -\frac{\hbar^2}{2m^*_{\mathrm{w,b}}(P)}\nabla^2 - \frac{e^2}{\varepsilon_{\mathrm{w,b}}(P)r} + V_{\mathrm{B}}(z,P) + |e|\,Fz\,, \tag{1}$$

where r is the carrier-impurity distance and subscripts w and b stand for the QW and barrier layer (BL) materials, respectively. $m^*_{\mathrm{w,b}}$ and $\varepsilon_{\mathrm{w,b}}$ are the conduction effective-masses and dielectric constant, respectively. V_{B} is the barrier potential which confines the donor electron in the QW

$$V_{\mathrm{B}}(P,T,z) = \begin{cases} 0 & \text{for} \quad |z| \le L(P)/2 \\ V_0(P,T) & \text{for} \quad |z| \ge L(P)/2\,, \end{cases} \tag{2}$$

where

$$V_0(P,T) = \begin{cases} \Gamma_{\mathrm{b}}(P,T) - \Gamma_{\mathrm{w}}(P,T) & \text{for} \quad P \le P_1 \\ \mathrm{X}_{\mathrm{b}}(P,T) - \Gamma_{\mathrm{w}}(P,T) + S_0 x (P-P_1)/P & \text{for} \quad P_1 < P \le P_2\,, \end{cases} \tag{3}$$

with P_1 the crossover pressure between the X_{b} conduction band and the Γ_{b} band, P_2 the crossover pressure between the X_{b} conduction band and the Γ_{w} band [1–4, 6]. Image charges are not considered in this model.

The trial wave function for the ground state is chosen as the product between the exact solution for the Hamiltonian in Eq. (1) without the impurity potential term at the right (with eigenvalue E_0) and the 1s-like hydrogenic wave function [10, 11].

The donor binding energy is calculated from the definition

$$E_{\mathrm{b}} = E_0 - E_{\mathrm{min}}\,, \tag{4}$$

where E_{min} is the eigenvalue for the Hamiltonian in Eq. (1) with the impurity potential term, minimized with respect to the variational parameter.

3. Results and discussion In Fig. 1 results are presented for the binding energy as a function of the impurity position for a GaAs–GaAlAs QW, dimensions 100 and 200 Å, with varying pressure and electric field. The electric field is pointing towards the $+z$ direction. By looking at just one of the curves, e.g., P = 10 kbar, F = 100 kV/cm, as a function of the z-position it is seen that at the positive boundary of the well the binding energy takes the lowest value. This is due to the fact that the electron cloud is closest to the $z = +L/2$ wall and the electric field can deform it almost without the interference of the opposite boundary. As the impurity moves to the left the electron cloud gets closer to the impurity site increasing the binding energy as a consequence of the boundary wall at $z = -L/2$ which does not allow the carrier to move beyond that point. This situation reaches a point where the electron is closest to the impurity site, giving a maximum in the binding energy, due to the field pulling the electron to the left, the left wall impeding its motion, and the motion of the impurity to the left.

Consider now a pair of curves corresponding to increasing pressure and constant electric field [17]. When the impurity site is in the region close to the $z = -L/2$, the binding energy is larger for the higher pressure where the electron cloud is more delocalized [see the inset in Fig. 1b], with respect to the lower pressure, due to the simultaneous effects of the lower barrier height, applied electric field and hydrostatic pressure which leads to remarkable different probability densities shown in the inset of Fig. 1b. Impurity positions, with constant F, close to the $z = +L/2$ wall give rise to similar binding energies. This is due to the shape of the binding energy as a function of pressure as shown in Ref. [17], Fig. 1, which shows that the binding energy takes similar values at the pressures 10 and 30 kbar. For the pair of curves with con-

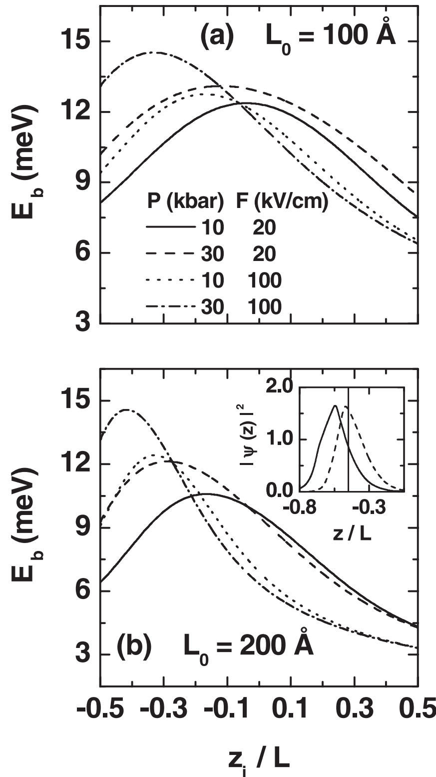

Fig. 1 Binding energy as a function of the impurity position along the growth direction for shallow-donor impurities in GaAs–(Ga, Al)As quantum wells. Some different values for the well thickness, hydrostatic pressure, and applied electric field are considered. The inset in Fig. 1b shows the probability density for an impurity at $z = -0.4L$. Dashed line corresponds to 10 kbar and solid line for 30 kbar.

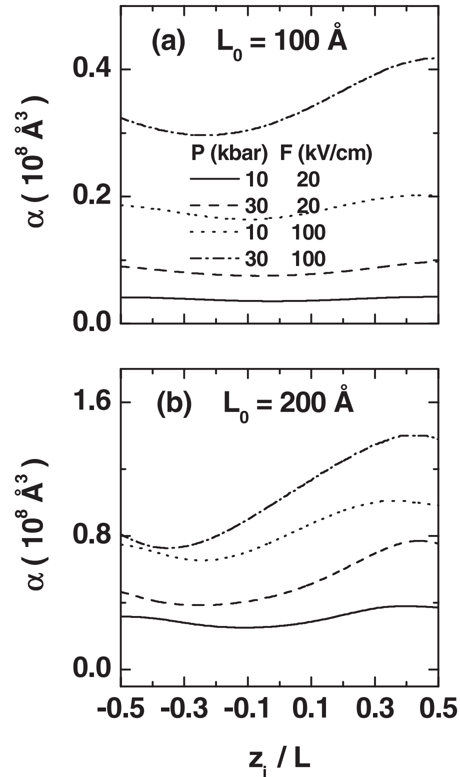

Fig. 2 Shallow-donor polarization as a function of the impurity position along the growth direction for impurities in GaAs–(Ga, Al)As quantum wells. Dimensions of the structure, hydrostatic pressure, and applied electric field are the same than those from Fig. 1.

stant pressure and increasing electric field, the binding energy maximum also moves closer to the negative side of the well for the higher applied electric field. The maximum binding energy value corresponds to the higher values of pressure and electric field.

Our results for the impurity polarizability are given in Fig. 2. The polarizability curves, for both dimensions, behave quite similarly. They take the higher values at the right side of the well where the electron cloud can be deformed easily by the electric field and then decrease as the opposite barrier starts to impede the carrier motion by the electric field action. This behavior is, of course, related to the binding energy results discussed above, i.e., at the right boundary the electron cloud is at its largest distance from the impurity site resulting in a small binding energy value and a large polarizability value. The minimum of the polarization curves roughly coincides with the maximum in binding energy. After the minimum polarizability value the curves slightly rise towards the left well barrier, this is related with the positioning of the electron cloud to the right of the impurity mentioned above. The magnitude of the polarizability is larger for $L = 200$ Å due to the fact that the electron cloud is more delocalized in this case. The polarizability magnitude is also larger for the higher pressure and electric field values for the reason that the electron cloud in the well becomes more delocalized and consequently more deformable [17].

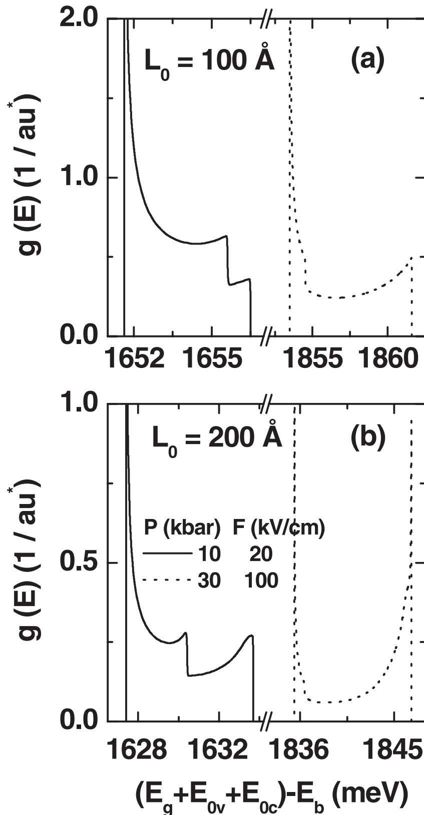

Fig. 3 Density of impurity states as a function of the effective GaAs–(Ga, Al)As quantum well gap and shallow-donor impurity binding energy difference. Some different values for the well thickness, hydrostatic pressure, and applied electric field are considered.

Finally, the DOIS produced by a uniform distribution of impurities along the length of the well is plotted in Fig. 3. The energy scale corresponds to the energy difference between the effective energy gap for the QW and the binding energy for donor impurities. The main feature is the presence of three peaks, as in the case of applying only an electric field, slightly shifted by the applied pressure. The applied electric field breaks the well mirror symmetry [10, 11] and produces an unsymmetrical electron binding energy as a function of the impurity position leading to a three-peak DOIS. The further application of a hydrostatic pressure moves the peak structure to higher energies.

4. Conclusions The simultaneous effect of pressure and electric field produces an electron binding energy trend, as a function of the impurity position, similar to the one obtained by the application of an electric field alone. The pressure effect is then to produce an additional displacement of the binding energy in the opposite direction to the applied electric field.

The polarizability follows the binding energy variation closely, i.e., when the impurity electron cloud is farthest from the impurity site the binding energy is the smallest, and the system is at its maximum deformation leading to the highest value of polarizability. The polarizability decreases as the impurity moves in the opposite direction to the electric field, where the electron cloud is more confined by the electric field and pressure effects.

The DOIS is a direct consequence of the binding energy variation with impurity position, which shows an asymmetrical profile leading to a three-peak structure, which could be use in valence–to–donor absorption experiments to tune the peaks to specific values or as a pressure detector.

Acknowledgements We are grateful to the Universidad de Antioquia (CODI) for the financial support. This work was partially financed by Colciencias, the Colombian Scientific Agency, under the grant number 1115-05-11502.

References

[1] H. J. Ehrenreich, J. Appl. Phys. **32**, 2155 (1961).
[2] D. E. Aspnes, Phys. Rev. B **14**, 5331 (1976).
[3] S. Adachi, J. Appl. Phys. **58**, R1 (1985).
[4] D. J. Wolford and J. A. Bradley, Solid State Commun. **53**, 1069 (1985).
[5] M. Chandrasekhar and H. R. Chandrasekhar, High Press. Res. **9**, 57 (1992).
[6] J. H. Burnett, H. M. Cheong, W. Paul, E. S. Koteles, and B. Elman, Phys. Rev. B **47**, 1991 (1993).

[7] M. Chandrasekhar and H. R. Chandrasekhar, Philos. Mag. B **70**, 369 (1994).
[8] A. M. Elabsy, Physica Scripta **48**, 376 (1993); Superlattices Microstruct. **14**, 65 (1993); J. Phys.: Condens. Matter **6**, 10025 (1994).
[9] H. O. Oyoko, C. A. Duque, and N. Porras-Montenegro, J. Appl. Phys. **90**, 819 (2001).
[10] J. López-Gondar, J. d'Albuquerque e Castro, and L. E. Oliveira, Phys. Rev. B **42**, 7069 (1990).
[11] R. B. Santiago, L. E. Oliveira, and J. d'Albuquerque e Castro, Phys. Rev. B **46**, 4041 (1992).
[12] K. F. Ilaiwi, Superlattices Microstruct. **20**, 173 (1996).
[13] H. Thien Cao and D. B. Tran Thoai, Solid State Commun. **97**, 643 (1996).
[14] V. Narayani and B. Sukumar, Solid State Commun. **90**, 579 (1994).
[15] C. A. Duque, A. Montes, and A. L. Morales, Physica B **302/303**, 84 (2001).
[16] N. Porras-Montenegro, S. T. Pérez-Merchancano, and A. Latgé, J. Appl. Phys. **74**, 7624 (1993).
A. Montes, C. A. Duque, and N. Porras-Montenegro, J. Phys.: Condens. Matter **10**, 5351 (1998).
[17] A. L. Morales, A. Montes, S. Y. López, and C. A. Duque, J. Phys.: Condens. Matter **14**, 987 (2002).